Performance Analysis of High-dimensional NOMA system with In-Phase/ Quadrature Index Modulation

Zhi xiang Wang
School of Electronics & Information
Soochow University
Suzhou, China
782161565@qq.com

Jia Hou[1,2]
1. Yangtze Delta Region Instituteame (Quzhou), University of Electronic Science and Technology of China
2. *School of Electronics & Information*
Soochow University
Suzhou, China
houjia@sude.edu.cn

***Abstract*—In this paper, a Non-orthogonal multiple access (NOMA) system based on High-Dimensional signals with In-Phase/Quadrature Index Modulation (HD-IQ-IM-NOMA) is proposed. At the transmitter, two users with the high-dimensional signal constellations are separated their coordinate values into two parts, which are respectively mapped to the active in-phase component subcarriers and the active quadrature component subcarriers in each OFDM subblock. Further, different transmit powers are allocated to the high-dimensional modulated signals of two users, and then superimposed by the OFDM subcarrier module to form a NOMA transmit signal. At the receiver, the maximum likelihood (ML) and successive interference cancellation (SIC) detection methods are considered. The simulation results demonstrate that the proposed scheme exhibits superior error performance compared to the traditional IM-NOMA systems.**

Keywords—NOMA, HD signals, index modulation (IM), ML detector, BER

I. INTRODUCTION

Non-orthogonal multiple access (NOMA) has received considerable attention as a candidate multiple access technology of LTE, 5G and beyond systems. Using NOMA, multiple terminals are jointly scheduled and share the same radio resource in time, frequency or code domain [1]. Unlike the traditional orthogonal multiple access (OMA) technology, NOMA allows multiple users to transmit data on the same subcarrier, which improves spectral efficiency [2-4].

Otherwise, in recent years, index modulation (IM)[5] has attracted widespread attention due to its advantages in improving energy efficiency, spectral efficiency, and error bit performance and it has been widely used in various systems, such as OFDM [6], which is called orthogonal frequency division multiplexing with index modulation (OFDM-IM). In order to reduce the bit error rate of the system, more studies have been conducted to increase the diversity of the system by introducing schemes such as coordinate interweaving [7]. In [8], a new IQ-IM-based OFDM system (HD-OFDM-IQ-IM) using HD signal constellation is proposed. Flexible transmission waveform design and the introduction of high-dimensional signal constellation with increased MED is helpful to improve the system's error performance. Meanwhile, IQ-IM is used to obtain more index bits, which improves the spectral and energy efficiency of the transmission system. At the same time, inspired by IM and classic OFDM-NOMA, a novel OFDM with IM based on NOMA (OFDM-IM NOMA) [9] is proposed, which innovatively combined IM technology with NOMA system. In this scheme, different users are allowed to share available resources more efficiently and flexibly. At present, most studies focus on designing detection algorithm with lower complexity for OFDM-IM NOMA system [10], and designing a "two-stage log-likelihood ratio LLR" detector to reduce the computational complexity of OFDM-IM NOMA. However, there are not many researches on reducing the bit error rate of OFDM-IM NOMA system.

This paper aims to improve the error performance of NOMA users in OFDM-IM NOMA system. Considering that the error performance of the system is improved by introducing HD signal to increase MED and the increase in the number of index bits generated by in-phase/orthogonal index modulation in [8], HD-OFDM-IQ-IM is introduced into the OFDM-IM NOMA system and the HD-IQ-IM-NOMA system model is proposed.

The main contributions of this paper can be summarized as follows:

- Compared with the traditional OFDM-IM NOMA, the HD-IQ-IM-NOMA system in this paper introduces the HD-OFDM-IQ-IM scheme, uses HD signal to enhance the MED between modulation symbols, and introduces in- phase/quadrature index modulation to improve the proportion of user index bits.
- The ML detector is used. When the spectral efficiency of the two users is equal, the complexity of the ML detection is similar to that of the conventional one. Meanwhile, the theoretical BER formula of two users under the system model are derived.
- Different NOMA users can share the same spectrum resources more flexibly.

II. SYSTEM MODEL

The structure of the proposed HD-IQ-IM-NOMA transmitter is illustrated in Fig.1. There is a base station (labeled as BS) and two users (labeled as U_1 for the near user and U_2 for the far user). All nodes are equipped with a single antenna. Assume that only the statistical CSI (Channel State Information) is known at the transmitter, while full CSI is available at the user side. That is, the user side could get the perfect channel estimate, although this is not possible.

For each user, a total of m_u $(u \in 1,2)$ bits are transmitted. Since the same procedures are applied for signal generation of each user, considering one user, m_u bits are divided into G subblocks, with each subblock containing p_u bits, where $p_u = m_u / G$. The p_u bits are mapped into subblocks with sizes n , $n = N / G$ and N

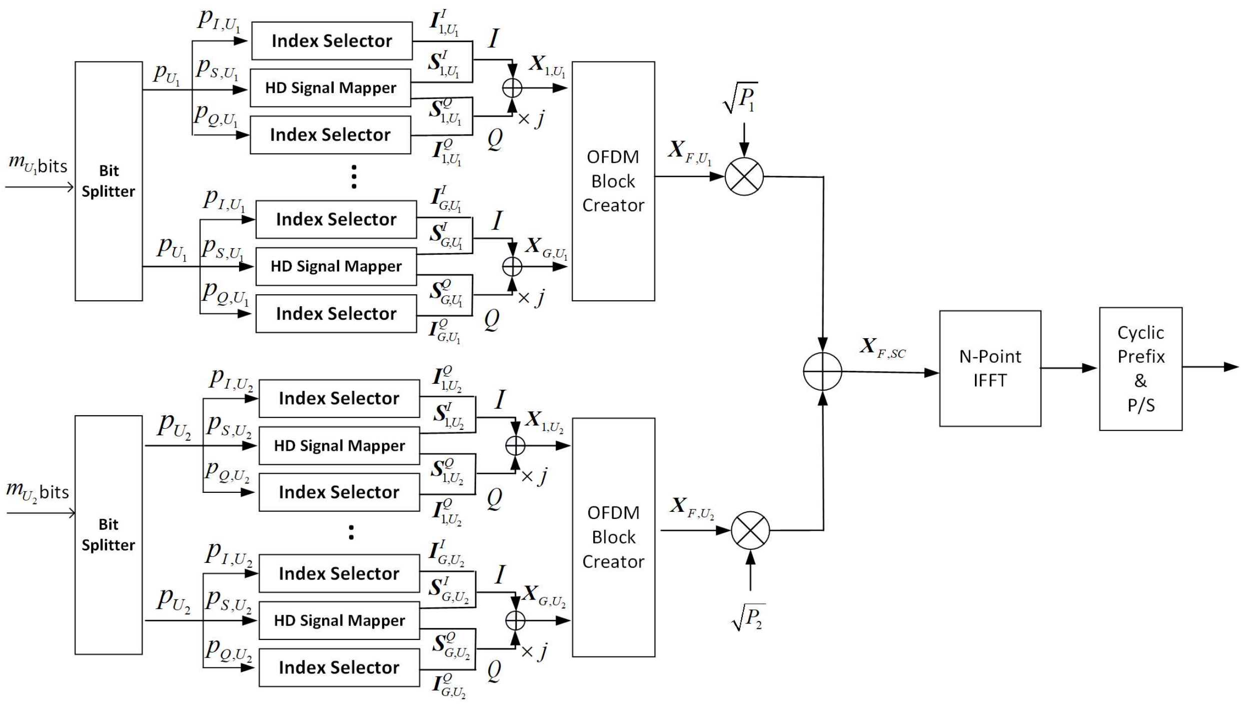

Fig. 1. The structure of HD-IQ-IM-NOMA transmitter.

represents the number of total subcarriers, that is, the size of fast Fourier transform (FFT), while n is the number of subcarriers in each subblock. The p_u bits are divided into three parts: $p_{I,u}$, $p_{Q,u}$, $p_{S,u}$. The index bits $p_{I,u}$ is used to activate the in-phase component of k_u subcarriers from n subcarriers to transmit the first k_u elements of the modulated symbol of user u . Thus, $p_{I,u} = \lfloor \log_2 C(n,k_u) \rfloor$, where $C(n,k_u)$ represents the binomial coefficient, and $\lfloor \cdot \rfloor$ is the floor function. The index bits $p_{Q,u}$ is used to activate the quadrature component of $D_u - k_u$ subcarriers from n subcarriers to transmit the last $D_u - k_u$ elements of the modulated symbol of u . Thus, $p_{Q,u} = \lfloor \log_2 C(n, D_u - k_u) \rfloor$, where D_u is the dimension of the high-dimensional signal constellation of user u , which adopted in this paper is obtained according to the design method in [8]. A D_u dimensional symbol $\boldsymbol{S}_D$ of a high-dimensional signal with size M_u can be represented as a column vector $(v_1 ... v_d ... v_D)^T$, $1 \le d \le D_u$ and the superscript T denotes transposition. The coordinate value of v_d is a nonzero real number used to distinguish whether the subcarrier component is activated or not. Therefore, $p_{S,u} = log_2 M_u$. Thus, the total number of bits transmitted by one sub-block is:

$$p_u = p_{I,u} + p_{S,u} + p_{Q,u} \tag{1}$$

According to [8], the generation method of modulation signal in Table I, ignore the subscript u , $\boldsymbol{I}_{Re}$ represents the selection mode of the in-phase component, and $\boldsymbol{S}_{Re}$ represents the data of the in-phase component of n subcarriers, and $\boldsymbol{I}_{\mathrm{Im}}$ represents the selection mode of the quadrature component, and $\boldsymbol{S}_{\mathrm{Im}}$ represents the data of the quadrature component of n subcarriers, the output signal of the ξ^{th} $(\xi \in \{1,...,G\})$ subblock of user u can be expressed as $\boldsymbol{X}_u^{\xi} = \boldsymbol{S}_{Re,u}^{\xi} + j\boldsymbol{S}_{Im,u}^{\xi}$,

TABLE I A LOOK-UP TABLE FOR HD-OFDM-IQ-IM (4,2,2)

p_I	$\boldsymbol{I}_{Re}$	$\boldsymbol{S}_{Re}$	p_Q	$\boldsymbol{I}_{\mathrm{Im}}$	$\boldsymbol{S}_{\mathrm{Im}}$
00	$\{1,2\}$	$[v_1\, v_2\, 0\, 0]$	00	$\{1,2\}$	$[v_3\, v_4\, 0\, 0]$
01	$\{2,3\}$	$[0\, v_1 v_2\, 0]$	01	$\{2,3\}$	$[0\, v_3 v_4\, 0]$
10	$\{3,4\}$	$[0\, 0\, v_1 v_2]$	10	$\{3,4\}$	$[0\, 0\, v_3 v_4]$
11	$\{1,4\}$	$[v_1\, 0\, 0\, v_2]$	11	$\{1,4\}$	$[v_3\, 0\, 0\, v_4]$

where $j = \sqrt{-1}$. Connecting all subblocks at the OFDM-IM block generator, the OFDM-IM signal in the frequency domain can be represented as:

$$\boldsymbol{X}_{F,u} = [\boldsymbol{X}_u^1\, \boldsymbol{X}_u^2 ... \boldsymbol{X}_u^G]^T \tag{2}$$

where F represents the frequency domain and $u \in \{1,2\}$ represents different users. The superimposed signal transmitted by multiplexing different users' frequency domain signals, which are modulated in the same way and then combined using superposition coding (SC) technique for simultaneous transmission and power-domain multiplexing, can be represented as:

$$\boldsymbol{X}_{F,SC} = \sqrt{\alpha P_{BS}}\boldsymbol{X}_{F,1} + \sqrt{(1-\alpha)P_{BS}}\boldsymbol{X}_{F,2} \tag{3}$$

where P_{BS} and α are the total transmission power (per subcarrier) of the base station (BS) and the power allocation factor, respectively. Considering $P_{BS} = 1$ and $0 \le \alpha \le 1$, the average power of the near user and the far user are respectively: $P_1 = \alpha P_{BS}$ and $P_2 = (1-\alpha)P_{BS}$.

Subsequently, the superimposed signal in the frequency domain is transformed into the time domain by the inverse fast Fourier transform (IFFT) to obtain the time-domain signal.

$$\boldsymbol{X}_{T,SC} = IFFT\{\boldsymbol{X}_{F,SC}\} = [x_0\, x_1 \ldots x_{N-1}]^T \tag{4}$$

where T represents the time domain. After the IFFT operation, a cyclic prefix of length L, $[x_{N-L}\, x_{N-L+1} \ldots x_{N-1}]^T$, is added to the front of the time-domain signal, and then the signal is sent to the channel after parallel-to-serial (P/S) conversion for transmission. The signal is transmitted through a frequency-selective Rayleigh fading channel, which can be represented by the channel impulse response (CIR) coefficients:

$$\boldsymbol{t} = [t(0)t(1)\ldots t(v-1)]^T \tag{5}$$

where $t(\varphi), \varphi = 0,\ldots,v-1$, are circularly symmetric complex Gaussian random variables with $CN(0,1/v)$ distribution, and v is the number of propagation paths. Assuming that the channel remains constant during the transmission of the OFDM block, and the length L of the cyclic prefix (CP) is greater than v, the received vectors of the two users can be given by the following equation:

$$\boldsymbol{y}_u = \boldsymbol{H}_u \boldsymbol{X}_{F,SC} + \boldsymbol{w}_u = [y_u(0)\ldots y_u(N-1)]^T \tag{6}$$

where $\boldsymbol{H}_u = diag(\boldsymbol{h}_u) = diag([h_u(0)\ldots h_u(N-1)]^T)$ and $\boldsymbol{w}_u = [w_u(0)\ldots w_u(N-1)]^T$ are the channel matrix and the noise vector for the two users in the frequency domain, respectively, and $diag(\cdot)$ converts a vector into a diagonal matrix. The distributions of $h_u(\beta)$ and $w_u(\beta)$ are $CN(0,\sigma_u^2)$ and $CN(0,N_0)$, respectively, where N_0 is the noise variance in the frequency domain. Due to the difference in distance between the near user and the far user, it can be assumed that the channel gain of the near user is greater than that of the far user $(\sigma_1^2 \geq \sigma_2^2)$.

At the receiver side, after serial-parallel conversion (S/P), CP removal and fast Fourier transform (FFT), the received time domain signal is converted to the frequency domain signal $\boldsymbol{y}_u$. For subblock ξ, the receiver uses the ML detector to consider all possible cases and make a joint hard decision that includes both the in-phase and quadrature index bits and the $\boldsymbol{S}_D$ symbol. For two users, the set of all possible subblocks is defined as: $\boldsymbol{B}_u = \{\boldsymbol{b}_{u,0}, \boldsymbol{b}_{u,1}, \ldots, \boldsymbol{b}_{u,2^{p_u}-1}\}$ and the total number of possible subblocks as 2^{p_u}.

Far User(U_2): Since the signal power of the far user is higher than the near user $(\alpha < 0.5)$, the U_1 signal is treated as interference, and an ML detector is used to directly demodulate the U_2 received signal. Using the set $\boldsymbol{B}_2$, The estimate of the index bits and transmitted S_D symbol is determined by minimizing the following metric:

$$\hat{\boldsymbol{x}}_2^{\xi} = \arg\min_{\boldsymbol{b}_2 \in \boldsymbol{B}_2} \left\| \boldsymbol{y}_2^{\xi} - \sqrt{P_2}\boldsymbol{H}_2^{\xi}\boldsymbol{b}_2 \right\|_F^2 \tag{7}$$

where $\boldsymbol{y}_2^{\xi} = [y_2(n(\xi-1))\ldots y_2(n\xi-1)]^T$ are the received signal vector of the ξ^{th} subblock of U_2, and $\boldsymbol{H}_2^{\xi} = [h_2(n(\xi-1)\ldots h_2(n\xi-1)]^T$ are the channel matrix of the ξ^{th} subblock of U_2, respectively.

Near User(U_1): Since the signal power of the near user is less than the far user $(\alpha < 0.5)$, first the U_2 signal is decoded through SIC. In subblock ξ, using the set $\boldsymbol{B}_2$, an ML detector is used as follows:

$$\hat{\boldsymbol{x}}_{2,SIC}^{\xi} = \arg\min_{\boldsymbol{b}_2 \in \boldsymbol{B}_2} \left\| \boldsymbol{y}_1^{\xi} - \sqrt{P_2}\boldsymbol{H}_1^{\xi}\boldsymbol{b}_2 \right\|_F^2 \tag{8}$$

where $\boldsymbol{y}_1^{\xi} = [y_1(n(\xi-1))\ldots y_1(n\xi-1)]^T$ and $\boldsymbol{H}_1^{\xi} = [h_1(n(\xi-1)\ldots h_1(n\xi-1)]^T$ are the received signal vector and channel matrix, respectively, for sub-block ξ of the near user U_1. The decoded U_2 signal is then reconstructed as follows:

$$\hat{\boldsymbol{z}}_2 = [\hat{\boldsymbol{x}}_{2,SIC}(1)\ldots\hat{\boldsymbol{x}}_{2,SIC}(G)]^T \tag{9}$$

Subtract it from the total received signal as follows:

$$\boldsymbol{r}_1 = \boldsymbol{y}_1 - \sqrt{P_2}\boldsymbol{H}_1\hat{\boldsymbol{z}}_2 = [r_1(0)\ldots r_2(N-1)]^T \tag{10}$$

Hence, the interference of the U_2 signal on the U_1 signal is eliminated. Finally, the U_1 signal is decoded by ML-based detection rule with the U_1 subblock set $\boldsymbol{B}_1$:

$$\hat{\boldsymbol{x}}_1^{\xi} = \arg\min_{\boldsymbol{b}_1 \in \boldsymbol{B}_1} \left\| \boldsymbol{r}_1^{\xi} - \sqrt{P_1}\boldsymbol{H}_1^{\xi}\boldsymbol{b}_1 \right\|_F^2 \tag{11}$$

where $\boldsymbol{r}_1^{\xi} = [r_1(n(\xi-1))\ldots r_2(n\xi-1)]^T$ are the interference-free signal vector for subblock ξ of the near user U_1. In the context of plural multiplication as the cardinality base, for user U_2, in the case of direct decoding, the computational complexity of the ML detector for each sub-block in (7) is $O(2^{p_{I,2}}2^{p_{Q,2}}M_2)$, as $\boldsymbol{B}_2$ involves implementing $2^{p_{I,2}}2^{p_{Q,2}}M_2$ different sub-blocks. At user U_1, the signal from user U_2 is first decoded, and then the signal of user U_1 is decoded from the reconstructed signal. The computational complexity of ML detectors in (8) and (11) is $O(2^{p_{I,2}}2^{p_{Q,2}}M_2)$ and $O(2^{p_{I,1}}2^{p_{Q,1}}M_1)$. Therefore, the computational complexity of an ML detector near user U1 is $O(2^{p_{I,1}}2^{p_{Q,1}}M_1 + 2^{p_{I,2}}2^{p_{Q,2}}M_2)$. As in [9], the computational complexity of the ML detector for the far user in traditional OFDM-IM NOMA is $O(2^{p_2}2^{k_2}M)$, and the near user also uses successive interference cancellation (SIC) for decoding. Therefore, the computational complexity of the ML detector for the near user is $O(2^{p_2}2^{k_2}M + 2^{p_1}2^{k_1}M)$. When the spectral efficiency of the two schemes is the same, the computational complexity of the user's ML detection algorithm is the same, but the BER performance of the user will be improved because the ratio of index bits is increased in this paper.

III. PERFORMANCE ANALYSIS

A. Theoretical BER derivation

In this subsection, a theoretical analysis is conducted on the error rate performance of two users. Using ML detector at the receiver side, the error performance of the scheme for two users can be estimated by the paired error probability (PEP) of a single subblock. For simplicity, the subblock index ζ is omitted.

From (6), supposed that $\widehat{\boldsymbol{X}}_u = diag(\hat{\boldsymbol{b}}_u)$ is the error event for $\boldsymbol{X}_u = diag(\boldsymbol{b}_u)$, in this case, the unconditional PEP (UPEP) can be calculated as in [8]

$$P(\boldsymbol{X}_u \to \widehat{\boldsymbol{X}}_u) = \frac{1/12}{\det(\boldsymbol{I}_n + q_1\boldsymbol{K}_n\boldsymbol{A})} + \frac{1/4}{\det(\boldsymbol{I}_n + q_2\boldsymbol{K}_n\boldsymbol{A})} \tag{12}$$

where $\boldsymbol{I}_n$ is the $n \times n$ identity matrix and $\det(\cdot)$ is the determinant of the matrix. $\boldsymbol{A} = (\boldsymbol{X}_u - \widehat{\boldsymbol{X}}_u)(\boldsymbol{X}_u - \widehat{\boldsymbol{X}}_u)^H$, where $(\cdot)^H$ denotes Hermitian transposition. $\boldsymbol{K}_n = E\{\boldsymbol{h}_u\boldsymbol{h}_u^H\}$, denotes the expected channel coefficient. From (12), the error performance of a single subblock is directly affected by the expected $\boldsymbol{K}_n$ of the corresponding channel coefficient and the distance matrix $\boldsymbol{A}$ between $\boldsymbol{X}_u$ and $\widehat{\boldsymbol{X}}_u$.

The distance matrix $\boldsymbol{A}$ of the subblock is affected by the signal constellation used for the modulation symbol. The MED values of the utilized signal constellations are listed in Table II. At the same, a comparison is made with the MED of traditional 8QAM and 16QAM constellations. Table II shows that the MEDs of HD signal constellations are larger than the corresponding 2D ones. According to (12), the effect of using different constellations on the error performance of a single user is shown in Fig 2, in the area of high SNR, the use of high-dimensional signal constellation can improve the error performance of users.

After obtaining the UPEP of each user,, the average bit error probability (ABEP) can be approximated as

$$P_{b,U_1} \approx 0.5P_{S,U_2} + (1 - P_{S,U_2}) \times \frac{\sqrt{P_1}}{p2^p}\sum_{\boldsymbol{X}_1}\sum_{\widehat{\boldsymbol{X}}_1} P(\boldsymbol{X}_1 \to \widehat{\boldsymbol{X}}_1)e(\boldsymbol{X}_1 \to \widehat{\boldsymbol{X}}_1) \tag{13}$$

Where the P_{S,U_2} is

$$P_{S,U_2} = \frac{\sqrt{P_2}}{2^p}\sum_{\boldsymbol{X}_2}\sum_{\widehat{\boldsymbol{X}}_2} P(\boldsymbol{X}_2 \to \widehat{\boldsymbol{X}}_2) \tag{14}$$

is the symbol error probability (SEP) of the U_2 and $e(\boldsymbol{X}_u \to \widehat{\boldsymbol{X}}_u)$ stands for the number of bit errors for the corresponding pairwise error event $(\boldsymbol{X}_u \to \widehat{\boldsymbol{X}}_u)$. The interference of U_1 to U_2 signal is ignored, so the ABEP of U_2 can be approximated as

$$P_{b,U_2} \approx \frac{\sqrt{P_2}}{p2^p}\sum_{\boldsymbol{X}_2}\sum_{\widehat{\boldsymbol{X}}_2} P(\boldsymbol{X}_2 \to \widehat{\boldsymbol{X}}_2)e(\boldsymbol{X}_2 \to \widehat{\boldsymbol{X}}_2) \tag{15}$$

B. Optimum Power Allocation

It can be seen from (13) and (15) that the BER performance of the two users are affected by the power allocation factor α .Current NOMA literature mostly considers a fixed power allocation without any search method. In order to obtain better performance, in this subsection, the power allocation factor α is determined according to the average BER of both users using Monte Carlo simulation. Since the search algorithm of power allocation factor is not studied in this paper, this method as in [9] is only used as a reference to determine the value of power allocation factor α in this paper. For different k_1 and k_2 values, the performance of the users may vary, therefore, the average performance of the U_1 and U_2 is considered as in [9]:

$$Avg_{BER} = \frac{p_1 BER_1 + p_2 BER_2}{p_1 + p_2} \tag{16}$$

where BER_1 and BER_2 stand for the bit error rate of the U_1 and U_2, respectively. As shown in Fig. 3, under the condition of a fixed SNR of 30dB, using the 4D signal constellation, two different configurations are considered: 1) $k_1 = 1$ and $k_2 = 2$, 2) $k_1 = k_2 = 2$. With an increasing interval of 0.05 from $\alpha = 0$ to $\alpha = 0.5$, the BER of single user and the ABEP of two users under the two configurations are simulated. Select α with the lowest ABEP.

TABLE II THE MED OF THE UTILIZED SIGNAL CONSTELLATIONS

Constellation	**2D**	**3D**	**4*D***	**5*D***
M=8	0.8156	1.1547	1.4142	1.5492
M=16	0.6325	0.7559	1.0000	1.2649

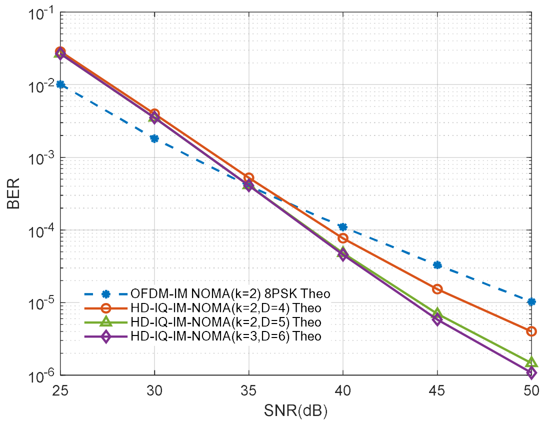

Fig. 2. Theoretical BER curves for individual user under different signal constellations

IV. SIMULATION AND NUMERICAL RESULTS

In order to compare the performance of OFDM-IM NOMA in [9], the parameters set in this paper are consistent with those set as in [9]: $N = 128, L = 16$ $\sigma_1^2 = 0dB, \sigma_2^2 = -3dB$. The average energy of each subcarrier is 1. Assuming that $n = 4$, and the number of activated subcarriers of the in-phase component is $k_1 = 2$ and $k_2 = 2$, respectively. The optimal power allocation factor $\alpha = 0.1$ can be obtained from the ABEP curve in Fig. 3.

In Fig. 4, the BER curves of two users under the two schemes of traditional OFDM-IM NOMA and the HD-IQ-IM-NOMA in this paper with the same n and k values. Under the same channel conditions, the simulation results show that the HD-IQ-IM-NOMA achieves significant error gain compared with the traditional OFDM-IM NOMA. This gain is particularly obvious in the high SNR region, where the SNR gain of U_1 and U_2 are both about 5dB at the BER of 10^{-4}. Moreover, in Fig. 4, the theoretical BER curves of two users, gradually approaches the simulation values. That mean, the theoretical curves obtained by (13) and (15) are approximations.

In Fig. 5, set $\sigma_1^2 = 0dB, \sigma_2^2 = -6dB$, the BER performance are different under different channel conditions. In $\sigma_1^2 = 0dB, \sigma_2^2 = -3dB$, the performance of U_1 is worse than that in $\sigma_1^2 = 0dB, \sigma_2^2 = -6dB$, but BER performance of U_2 is better. By setting different subcarrier parameters and power allocation factor, the performance of users will be affected.

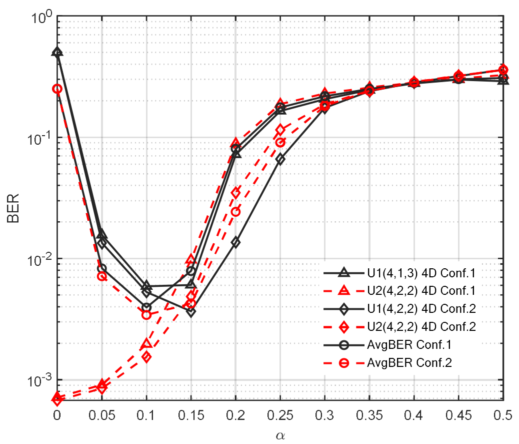

Fig. 3. Optimal α search from 0 to 0.5 for a fixed SNR of 30dB

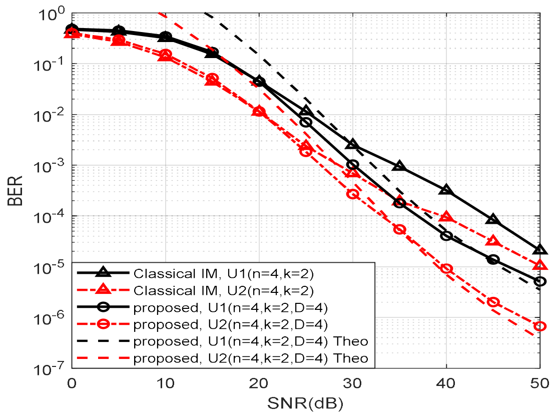

Fig. 4. Error performance of HD-IQ-IM-NOMA compared to traditional OFDM-IM NOMA

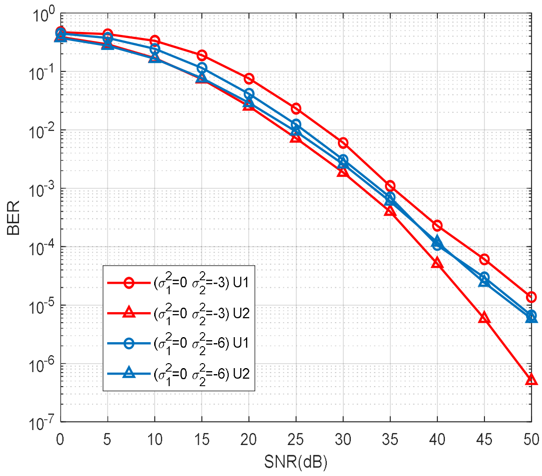

Fig. 5. the BER performance of users under different channel conditions

V. Conclusion

In this paper, the HD-OFDM-IQ-IM is applied for a power domain NOMA system, and the BER expression of the HD-IQ-IM-NOMA system model is derived. The use of HD signals and In-Phase/Quadrature Index Modulation could improve the proportion of user index bits, which allows NOMA users to obtain better error performance, while different users can more flexibly share the same spectrum resources.

Acknowledgment

This work was supported by NSFC, China (62071319).

References

[1] Makki, Behrooz, et al. "A survey of NOMA: Current status and open research challenges." IEEE Open Journal of the Communications Society 1 (2020): 179-189.

[2] Islam, SM Riazul, et al. "Power-domain non-orthogonal multiple access (NOMA) in 5G systems: Potentials and challenges." IEEE Communications Surveys & Tutorials 19.2 (2016): 721-742.

[3] Qian, Li Ping, et al. "Optimal SIC ordering and computation resource allocation in MEC-aware NOMA NB-IoT networks." IEEE Internet of Things Journal 6.2 (2018): 2806-2816.

[4] Kara, Ferdi, and Hakan Kaya. "BER performances of downlink and uplink NOMA in the presence of SIC errors over fading channels." IET Communications 12.15 (2018): 1834-1844.

[5] Kaddoum, Georges, Mohammed FA Ahmed, and Yogesh Nijsure. "Code index modulation: A high data rate and energy efficient communication system." IEEE Communications Letters 19.2 (2014): 175-178.

[6] Başar E, Aygölü Ü, Panayırcı E, et al. Orthogonal frequency division multiplexing with index modulation[J]. IEEE Transactions on signal processing, 2013, 61(22): 5536-5549.

[7] Başar, Ertuğrul. "OFDM with index modulation using coordinate interleaving." *IEEE Wireless Communications Letters* 4.4 (2015): 381-384.

[8] Chen Z, Lu Y, Kang S G. High-dimensional OFDM with in-phase/quadrature index modulation[J]. IEEE Access, 2021, 9: 44198-44206.

[9] Arslan, Emre, Ali Tugberk Dogukan, and Ertugrul Basar. "Index modulation-based flexible non-orthogonal multiple access." IEEE Wireless Communications Letters 9.11 (2020): 1942-1946.

[10] Li J, Li Q, Dang S, et al. Low-complexity detection for index modulation multiple access[J]. IEEE Wireless Communications Letters, 2020, 9(7): 943-947.